17th World Conference on Earthquake Engineering, 17WCEE
Sendai, Japan - September 13th to 18th 2020

Guidelines for Utilization of Site-Based Simulated Ground Motions for Performance-Based Earthquake Engineering of Ordinary Bridges

J. Fayaz[(1)], M. Dabaghi[(2)], F. Zareian[(3)]

[(1)] *PhD Candidate, Department of Civil and Environmental Engineering, University of California, Irvine, CA, USA, jfayaz@uci.edu*
[(2)] *Assistant Professor, Department of Civil and Environmental Engineering, American University of Beirut, Riad El-Solh, Beirut, Lebanon, md81@aub.edu.lb*
[(3)] *Associate Professor, Department of Civil and Environmental Engineering, University of California, Irvine, CA, USA, zareian@uci.edu*

Abstract

This study aims to harness the capability of synthetic ground motions for the design of standard ordinary bridges based on PBEE concepts. The outcome is a set of guidelines, that helps engineers generate ground motion time-histories for performance assessment of ordinary bridges in a standardized format. To develop the required knowledge for this purpose, site-specific synthetic ground motions representing 100,000 years are simulated for seven sites located in Southern California. Particularly the site-based simulation methods developed by Rezaeian and Der Kiureghian (2012) and Dabaghi and Der Kiureghian (2014) denoted as the DRD mode, is used in this study. The simulated site-based ground motions are then used to conduct Non-Linear Time-History Analysis (NLTHA) of four ordinary bridge structures for the seven sites leading to a total of 28 combinations. From this analysis, EDPs associated with ground motion Intensity Measure (IM) corresponding to the target design hazard (λ(IM)) is obtained and considered as the Point of Comparison (PoC). Using statistical procedures such as hypothesis testing and Kullback-Leibler (KL) Divergence, the number of ground motions that can replicate the mean value of PoC is obtained for all bridge and site combinations. The result of this study will assist engineers in making informed decisions in generating a proper set of ground motions and intercept angles for conducting the NLTHA of bridge structures.

Keywords: Ground Motion Simulation, Site-Based Synthetic Ground Motions, Ordinary Bridges, Statistical Tests

1. Introduction

Current Caltrans Seismic Design Criteria (SDC, ver. 1.7 – Apr. 2010 and ver. 2.0 – Apr. 2019), and state-of-practice, in general, are not well-suited to address Performance-based Earthquake Engineering (PBEE) concepts in the design of standard ordinary bridges. In essence, current SDC (SDC ver. 1.7 and ver. 2.0) states that standard ordinary bridges are "*expected to remain standing but may suffer significant damage requiring closure*" at the design level seismic event. Such a design philosophy fails to address issues such as safety, functionality, and durability of bridge structures; service life optimization and inclusion of lifecycle cost in decision making on the selection of "best" structural system and proportioning its components; and a holistic view of the transportation network and its performance as a whole. These issues, as addressed in California Bridges and Structures Strategic Direction, are foundational issues to any update to SDC and other design guidelines and tools for proportioning standard ordinary bridges. Such updates require that PBEE concepts become the cornerstone of Caltrans practice in the design of ordinary bridges. Within the PBEE framework, researchers have faced various challenges such as: identifying quanitiable and meaningful performance objectives, identifying representations of ground motion intensity that accurately represents the seismic hazard at the site, and the global bridge response characterization, and many others. The current challenge is to transfer the sophisticated research developments to the practicing engineers through applied but comprehensive procedures that facilitate efficient implementation. The first step for such implementation is the development of guidelines for modeling ground motion hazard that is tailored for the design and assessment of standard ordinary bridges for their respective site.

Current Caltrans design practice is based on utilizing design Acceleration Response Spectra (ARS) with a 5% probability of exceedance in 50 years. Conditioned on using nonlinear response history analyses for assessing the behavior of a bridge structure, engineers select 7 recorded or synthetic ground motions and adjust them to the desired, and adjusted (AASHTO, 2011), ARS curves using linear scaling or spectral matching. Such matching has few shortcomings: (1) it does not directly account for ground motion directionality, which may

arise due to near-fault effects such as rupture directivity and the fling step, (2) it fails to accurately address ground motion time-domain characteristics such as strong motion duration and velocity pulses in the scaling/adjustment routine, and (3) it does not directly discuss matching of two orthogonal components of ground motions in the proposed adjustments. These scaled ground motions are then applied in four orientations (0, 30, 60, and 90 degrees). For each orientation (and for each of the seven sets of time series), the peak response at each pertinent Degree of Freedom (DOF) is recorded. This leads to (4 orientations) x (7 sets of times histories) = 28 peak responses at each pertinent DOF. The bridge is then designed for the average of the recorded peak responses at each degree of freedom. The shortcomings of current Caltrans design practice in ground motion hazard representation, and the challenges that engineers face in selection and scaling of ground motion for PBEE of standard ordinary bridges can be overcome by utilizing synthetic ground motions. In the recent study conducted by a Caltrans research team (Yoon *et al.*, 2019), the concept of Probabilistic Damage Control Application (PDCA) was used to analyze the bridge structures using a site-based ground motion simulation model. The study proposed to use the event parameters of the top 3 contributing sources to simulate ground motions and then either conduct point scaling to match $S_a(T_1)$ of the Uniform Hazard Spectrum (UHS) or use range scaling method to match $S_a(T_1 \pm 1$ sec) of the Uniform Hazard Spectrum (UHS). However, this method has limitations as it adjusts the amplitude of simulated ground motion time series by applying linear scaling methods.

The simulation method utilized in this study is based on the site-based stochastic models of Rezaeian and Der Kiureghian (2012) and Dabaghi and Der Kiureghian (2018) - denoted as the DRD simulation model. The DRD model can be used to generate ground motions tailored for a location of interest and are fit to be used in a standardized format. This study aims to demonstrate the application of PBEE concepts using the DRD simulated ground motions. In doing so, it shows how to harness the capability of synthetic ground motions for the design of standard ordinary bridges based on PBEE concepts and in an applied and standardized format. Site-specific synthetic ground motion catalogs representing a time span of 100,000 years are simulated for seven sites located in Southern California. The simulated site-based ground motions are then used to conduct Nonlinear Time-History Analysis (NLTHA) of four ordinary bridge structures. The IMs and EDPs obtained for each ground motion catalog are used to calculate the IM hazard curves at each site and simulation-based EDP hazard curves for each bridge at each site. Rather than scaling the ground motions, among the synthetic ground motions that are simulated for the 100,000 years for a site, only the ground motions naturally possessing the IM value of the desired hazard level are selected, and their corresponding EDP values are used. Then, using various statistical procedures, a reduced sample number of ground motions that can replicate the statistics of this entire simulation set is proposed for the four ordinary bridges. This will assist engineers in making informed decisions in selecting an adequate number of ground motions and intercept angles for conducting the NLTHA of bridges.

2. Bridge Inventory

This study is focused on four Caltrans ordinary standard bridges. Four Reinforced Concrete (RC) ordinary bridge structures are selected as representatives for the statistical analysis. Table 1 includes the details of the four ordinary bridges with seat-type abutments which reflect the common bridge engineering practice in California. The first selected bridge is the *Jack Tone Road Overcrossing* (Bridge A) located at the city of Ripon, with two equal spans supported on a single column. The second bridge is the *La Veta Avenue Overcrossing* (Bridge B) located at the city of Tustin, with two equal spans supported on a two-column bridge bent. The third bridge is the *Jack Tone Road Overhead* (Bridge C) located at Ripon, with three equal spans and two three-column bridge bents. The fourth bridge is the curved bridge *E22-N55 Connector Over-crossing* (Bridge F) located in Santa Ana, with four equal spans supported on single columns. Finite Element models of the bridges are developed in OpenSees (McKenna *et al.* 2010). The seismic demand on a bridge is estimated by developing and analyzing a mathematical model of the superstructure and substructure of the bridge subjected to representative ground motions. The models represent the geometry, boundary conditions, mass distribution, energy dissipation as well as the interaction between elements. Since the bridge consists of many components that exhibit nonlinear behavior, a fully 3D nonlinear model is developed. The finite element

models are comprised of: seat-type abutments, abutment piles, shear keys, column bents, elastomeric bearing pads, backfill soil, and superstructure. The concrete and steel used in modeling possess a compressive strength f_c' = 5.0 *ksi* (34 *MPa*) with modulus of elasticity E_c = 4030.5 *ksi* (27.8 *GPa*) and yield strength = 65 *ksi* (448 *MPa*) with modulus of elasticity E_s = 29000 *ksi* (200 *GPa*). The finite element details of the bridges can be found in Fayaz *et al.* 2019.

Table 1- Characteristics of Bridge Structures

Bridge	**A**	**B**	**C**	**F**
Name	Jack Tone Road Overcrossing	La Veta Avenue Overcrossing	Jack Tone Road Overhead	E22-N55 Connector Over-crossing
Type	Straight	Straight	Straight	Curved
Total Length	220.6 ft	300.0 ft	418.0 ft	500.0 ft
Number of Spans	2	2	3	4
Column Bent	Single-column	Two-column	Three-column	Single-column
Column Radius	33.1 in	33.5 in	33.1 in	47.7 in
Column Height	22.0 ft	22.0 ft	24.1 ft	18.5 ft
Fundamental Period	0.61 sec	0.83 sec	0.79 sec	1.11 sec

3. Ground Motion Model

This study uses broadband site-based parameterized stochastic models to generate synthetic ground motions given information about the earthquake source, the site, and the source-to-site geometry hereafter referred to as Event Parameters. Compared to physics-based simulation models, site-based stochastic models are simpler, computationally efficient, and require fewer input parameters and that are easily accessible to engineers. In this study, the far-field model of Rezaeian and Der Kiureghian (2012) is used to simulate ground motions for sites with $R_{RUP} > 30$ km, and the near-fault model of Dabaghi and Der Kiureghian (2018) is used for near-fault sites with $R_{RUP} \leq 30$ km as it accounts for the rupture directivity effect. These two models are combinedly denoted as the DRD model. The model employs a modulated and filtered white-noise (MFW) process with time-varying filter parameters proposed by Rezaeian and Der Kiureghian (2008) and is able to represent the characteristics of recorded ground motions, including temporal and spectral non-stationarity and inherent variability. The near-fault model accounts for the occurrence of the forward rupture directivity effect in the form of a velocity pulse and produces pulse-like and non-pulse-like motions in accordance with their observed proportions among recorded motions. The model is formulated in terms of a relatively small number of physically meaningful model parameters that describe the ground motion amplitude, duration, and frequency content. The DRD model generates horizontal orthogonal pairs of synthetic ground motion time series for given Event Parameters that include type of faulting F ($= 0$ for strike-slip faults, $= 1$ for reverse and reverse-oblique faults), the moment magnitude M_w, the closest distance to rupture R_{RUP}, and the shear-wave velocity V_{s30} at the site. Also, for near-fault model, the depth to the top of the rupture plane (Z_{TOR}), and directivity parameters $s_{or}d$ and $\theta_{or}\phi$ (Dabaghi and Der Kiureghian, 2018) are required.

4. Site-Specific Simulations

Non-Linear Time-History Analysis (NLTHA) of the four ordinary bridge structures is conducted using simulated ground motions. In this study, site-specific synthetic ground motion catalogs representing a time span of 100,000 years are simulated for seven sites located in Southern California. The sites selected are a subset of the sites considered in the CyberShake study *15.12* (Graves *et al.* 2011); their coordinates and soil properties are listed in Table 2. The simulated catalogs represent the seismic hazard at each site. The evaluation of the seismic hazard at a site requires a seismic source model, which describes the geometry and magnitude of possible earthquake ruptures in a region of interest and their associated probabilities of occurrence over a specified time. The seismic source model used in this study is based on the mean Uniform California Earthquake Rupture Forecast, Version 2 (UCERF2) single branch model (Field *et al.* 2009). This version is

selected because all the necessary information about the ruptures is available in and can easily be extracted from the database of CyberShake study *15.12*. Note that CyberShake study *15.12* applies some modifications and additional constraints on UCERF 2, which are thus also applied in this study. These modifications include setting the minimum magnitude of considered earthquakes to 6, excluding background seismicity, and adjusting rupture areas for consistency with the simulation model (Graves *et al.* 2011). Moreover, for a specific site, only ruptures within 200 km of the site are considered in the hazard calculation. The ruptures are assumed to follow independent Poisson distributions with annual probabilities of occurrence provided in CyberShake. For each rupture, CyberShake also introduces a suite of variations in the hypocenter location and slip distribution, thus accounting for the natural variability in the rupture characteristics. This process results in an average of 415,000 rupture variations for each site.

Table 2- Coordinates, site conditions, number of relevant ruptures and ruptures variations from CyberShake, and number of events (and ground motions) in the simulated catalogs for the sites considered in this study

Site	**LADT**	**WNGC**	**PAS**	**SBSM**	**STNI**	**CCP**	**STG**
Latitude	34.052	34.042	34.148	34.065	33.931	34.055	33.664
Longitude	-118.257	-118.065	-118.171	-117.292	-118.179	-118.413	-117.769
V_{s30} Wills 2006 (m/s)	390	280	748	280	280	387	280
No. of relevant ruptures	7,019	7,076	7,155	7,076	7,001	6,939	6,793
No. of relevant rupture variations	476,920	478,210	484,943	478,210	475,910	475,065	464,072
Total No. of GMs in 100,000 year catalogs	10,406	10,663	10,492	10,663	10,102	10,046	10,696

A comprehensive list of all the possible earthquake rupture sources in the region of interest (about 15,000 ruptures) is obtained from the CyberShake platform. The platform provides a total of more than 800,000 different rupture variations in the region of study. For each site, Table 2 presents the number of relevant ruptures (those within 200 km) and rupture variations extracted from CyberShake. In summary, for this study, the source model is defined in terms of the geometry and magnitude of all the relevant ruptures, their annual probability of occurrence, and the variations in the hypocenter location for each rupture. This source information is sufficient to obtain all the Event Parameters that are necessary as input for simulating synthetic ground motions using the DRD model. Dabaghi *et al.* (2013) and Azar *et al.* (2019) described a simulation-based approach for performing probabilistic seismic hazard analysis (PSHA). The same methodology is used here to develop synthetic ground motion catalogs, calculate hazard curves, and obtain deaggregation results for the seven sites of interest. First, the UCERF2 seismic source model and Monte Carlo simulation are used to develop a synthetic catalog of earthquake scenarios (or events) over a period of $Y = 100{,}000$ years, by randomly sampling rupture variations according to their annual probability of occurrence. Next, for each of the seven sites and for each earthquake scenario, the corresponding Event Parameters F, M_w, Z_{TOR}, R_{RUP}, V_{s30}, $s_{or}d$, and $\theta_{or}\phi$ are obtained. Then the DRD ground motion model is used to generate at each site of interest one synthetic pair of horizontal ground motion time series for each scenario (or event) in the catalog. Because the DRD model was not fitted to earthquakes from normal faults, $F = 1$ is used for ground motions from normal and normal-oblique faults, *i.e.*, they are assumed to be similar to ground motions from reverse and reverse-oblique faults. This procedure results in one catalog of $Y = 100{,}000$ years at each of the seven sites. Each catalog represents a possible realization of the ground motions that may occur at the site over a duration of 100,000 years. Table 2 presents for these sites the number of events (or ground motions) in the simulated catalogs. Hazard curves and deaggregation results at each site are then calculated from these catalogs. The *RotD50* S_a (Boore *et al.* 2006) is the ground motion Intensity Measure (IM) used to develop the hazard curves.

Next, the hazard curves and deaggregation results obtained using the simulation-based approach are compared with those obtained using the U.S. Geological Survey (USGS) Unified Hazard Tool (UHT) (2008), which is widely used by engineers for seismic design or assessment studies at a site with known location and V_{s30}. The 2008 dynamic version of the USGS UHT is used in this study because it uses UCERF2 as the seismic source

model for California (Petersen *et al.* 2008). The 2008 USGS UHT uses as ground motion model the 2008 NGA GMPEs, namely Boore and Atkinson (2008), Campbell and Bozorgnia (2008), and Chiou and Youngs (2008), all weighted equally (Petersen *et al.* 2008). Theses GMPE models include terms for basin depth. The IM for which the 2008 USGS UHT hazard curves are calculated is the *RotD50* horizontal component of spectral acceleration. Note that the 2008 USGS UHT provides deaggregation and hazard curve results only for PGA and spectral periods of 0.2, 1, and 2 s, and only for V_{s30} values of 180, 259, 360, 537, 760 and 1150 m/s. For each site, the V_{s30} value nearest the one extracted from CyberShake is used in the UHT and is listed in Table 2.

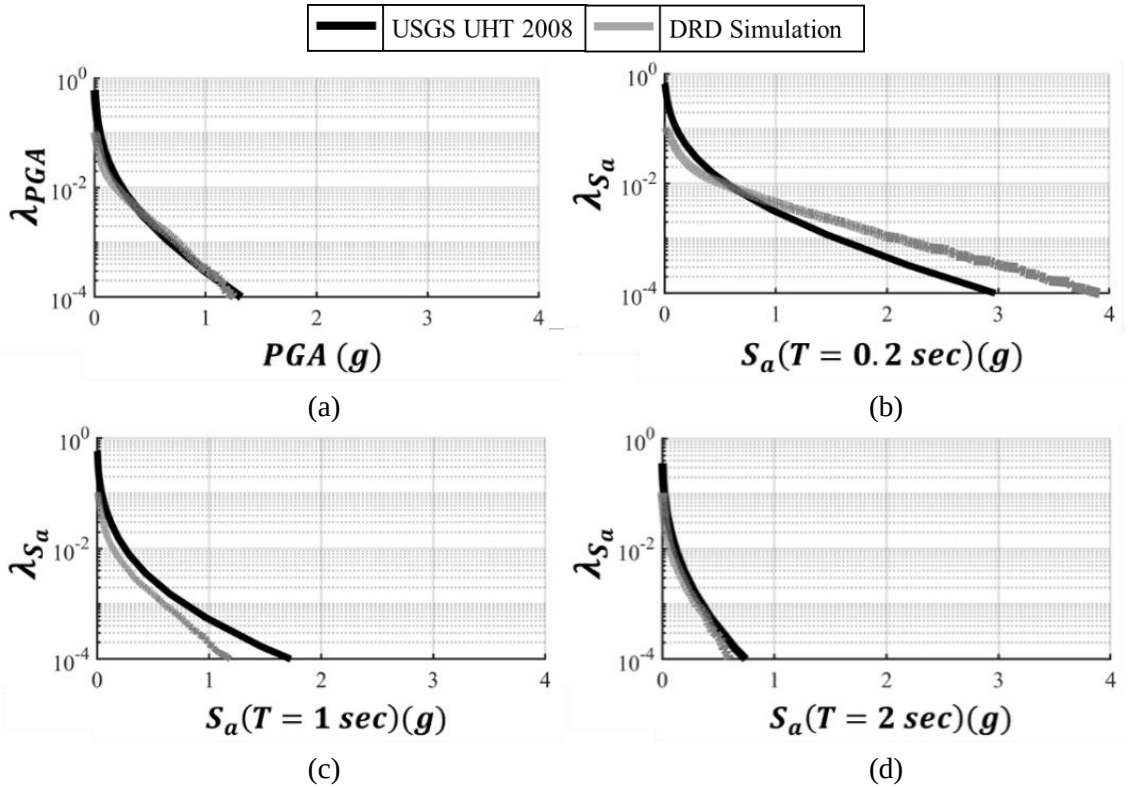

Fig 1- Hazard Curves Comparison for: (a) PGA level, (b) S_a at T=0.2 s, (b) S_a at T=1 s, and (d) S_a at T=2 s

Fig 1 compares the hazard curves obtained using the simulated $Y = 100{,}000$ year catalog at LADT with the hazard curves obtained from the 2008 USGS UHT. Comparisons are made for: (a) PGA level, (b) S_a at $T = 0.2$ s, (b) S_a at $T = 1$ s, and (d) S_a at T =2 s. Fig 1a shows that the PGA hazard curves are similar for both methods. However, some differences exist for the $S_a(T)$ hazard curves. At $T = 0.2$ s, the DRD simulation-based approach results in higher mean annual frequency values of $S_a(T = 0.2)$ compared to the USGS UHT; see Fig 1b. This is not the case at $T = 1$ s, where the mean annual frequency values of $S_a(T = 1.0)$ from the USGS UHT are higher; see Fig 1c. This difference could be due to an overestimation of ground motions levels by the DRD model for $T = 0.2$ s and an underestimation of these levels at $T = 1$ s compared with the 2008 NGA GMPEs. To interpret the differences, a deaggregation of the hazard at the high hazard levels are needed to determine the most contributing scenarios at that level and compare the ground motion levels predicted by the DRD model and the GMPEs. At $T = 2$ s, the results from both models are similar; see Fig 1d. Fig 2 shows the deaggregation into the contributing sources of the $S_a(T)$ hazard curves at $T = 1$ s and for a 5% probability of exceedance in 50 years from both the DRD simulation-based methodology and the USGS UHT. The contributing sources and their ordering are also generally consistent between the two methods; the sources contributing most to the hazard are Elysian Park (Upper) and Puente Hills (LA). Any differences in the hazard curves and deaggregation results between the two methodologies can be attributed to several factors. First, although both methods use UCERF2 as their seismic source model, the simulation-based approach excludes background seismicity and ruptures at distances greater than 200 km. Second, and most importantly,

differences exist in the ground motion models used by the two methods (2008 NGA GMPEs versus DRD model). For example, two out of the three 2008 NGA GMPEs used in the UHT include basin effects while the DRD model does not; and the DRD model includes the directivity effect while the 2008 NGA GMPEs lack this capability. Despite these differences, the simulated catalogs are deemed representative of the true hazard at the site for the analysis and discussion that follow.

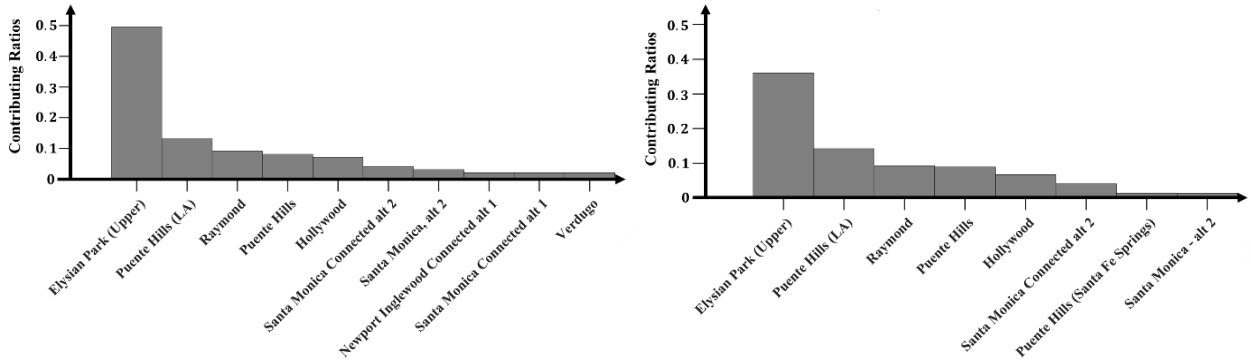

(a) (b)

Fig 2- Contributing Sources for deaggregation of S_a at 1 s using: (a) DRD Simulations, (b) USGS UHT

5. Statistical Analysis to Obtain Sample Number of Ground Motions and Intercept Angles for Proper Seismic Demand Estimation

The bi-directional synthetic ground motions simulated for the seven sites are used to conduct Nonlinear Time-History Analysis (NLTHA) of the four bridge structures. Due to asymmetry of the bridge structures, the two orthogonal components of the simulated ground motions are applied in incremental rotations from 0 to 180 degrees (excluding 180° for straight bridges) with *m* equal increments. For example, *m* = 6 implies that ground motion components are rotated in equally spaced 6 angles from 0° to 180°, which means ground motions are applied at 0°, 30°, 60°, 90°, 120°, and 150° with respect to the bridge`s longitudinal axis. The site-specific catalog simulations are conducted for *m* = 21 (*i.e.* intercept increment angle of 9 degrees). The behavior of ordinary bridge structures is mainly deduced by examining the maximum Column Drift Ratio (CDR) of the central bent throughout the time-history of ground motion. Hence, to be consistent with this practice and at the same time not to overestimate the EDPs, the EDP considered in this research is the median value of the maximum CDR obtained after applying the two components of ground motions at the *m* intercept angles. This EDP is termed as $Rot50CDR_m^i$ for i^{th} ground motion rotated at *m* uniformly spaced intercept angles and is expressed in Eq 1. It should be noted that the EDP of Column Drift Ratio (CDR) is termed in the form of *RotppEDP*, where *Rot* indicates the rotation of ground motion components, *pp* indicates the percentile value used for the measure (*e.g.* "00", "50" and "100" correspond to minimum, median and maximum values, respectively; the median value is used in this study), and *EDP* indicates that the measure is an Engineering Demand Parameter (*i.e.*, Column Drift Ratio *CDR*). Therefore, a total of approximately 5,880,000 (≈ 4 bridges × 7 sites × 10,000 ground motions × 21 intercept angles) NLTHA is conducted. Also, in this research, *Rot50CDR* should not be confused with *RotD50* spectral acceleration, *RotD50* is a measure of IM obtained after rotating the two ground motion components on SDOF and *Rot50CDR* is a measure of the EDP (Column Drift Ratio *CDR*) obtained after rotating the two components of ground motions on the MDOF bridge models. For the sake of brevity, in this study, the *RotD50* spectral acceleration at bridge's first mode period which is used as the primary IM of ground motions is termed as S_a or $S_a(T)$. Hence, each ground motion is associated with one value of $S_a(T)$ (IM) and one value of *Rot50CDR* (EDP).

$$Rot50CDR_m^i = median\left\{CDR^i_{0\times\frac{180^\circ}{m}} \quad CDR^i_{1\times\frac{180^\circ}{m}} \quad \cdots \quad CDR^i_{m\times\frac{180^\circ}{m}}\right\}^T \tag{1}$$

An example of *Rot50CDR* vs $S_a(T)$ for the catalog of simulated ground motions representing 100,000 years' time-span at the CCP site for Bridge A is given in Fig 3a. Similar plots for other sites are achieved by analyzing each bridge under their respective catalogs of simulated ground motions. It should be noted that the catalogs of the simulated ground motions do not only represent the S_a levels of the 100,000 years but also the other ground motion characteristics such as frequency content, time history evolution, duration, etc. Hence the EDPs obtained from these ground motions can be considered a good representation of the EDP hazard at the site. Since performing this type of simulation in design office can be quite cumbersome and would require heavy computational resources, this section aims to identify sample number (n) of hazard-targeted simulated ground motions which when applied in *m* uniformly spaced intercept angles, lead to sample EDPs that are statistically equivalent to the EDPs obtained using the whole catalog of site-specific ground motions at the target hazard level. The term 'hazard-targeted' in this context means ground motions that naturally possess the $S_a(T)$ of the target hazard level. The $S_a(T)$ associated with the target hazard level at the first mode period *T* is termed as $S_{a,haz}(T)$ where the hazard level in case of bridge designs is 5% in 50 years (975 years return period). The *Rot50CDR* EDPs corresponding to the $S_{a,haz}(T)$, obtained after conducting NLTHA using the catalog of ground motions, are termed as $Rot50CDR_{haz}$ and are assumed to follow a lognormal distribution with a mean $\mu_{Rot50CDR_{haz}}$ and standard deviation $\sigma_{Rot50CDR_{haz}}$. In order to obtain the statistics of $Rot50CDR_{haz}$, the *Rot50CDR* values associated with ground motions having $S_a(T)$ in the interval $S_{a,haz}(T) \pm 0.05g$ are used to compute the distribution parameters. An example of the selected values of *Rot50CDR* associated with $S_{a,haz}(T)$ for the CCP site for bridge A is given in Fig 3b (*i.e.*, shown with solid black dots). For each bridge, for all sites, various values of a sample number of ground motions (*n*) and intercept angles (*m*) are used in different combinations and, the obtained sample distribution parameters are then tested for statistical equivalency against a lognormal distribution with a mean $\mu_{Rot50CDR_{haz}}$ and standard deviation $\sigma_{Rot50CDR_{haz}}$. The *n* number of sample site-based ground motions are simulated such that they naturally possess a $S_a(T)$ equal to the $S_{a,haz}(T)$, however, differ in their other ground motion characteristics.

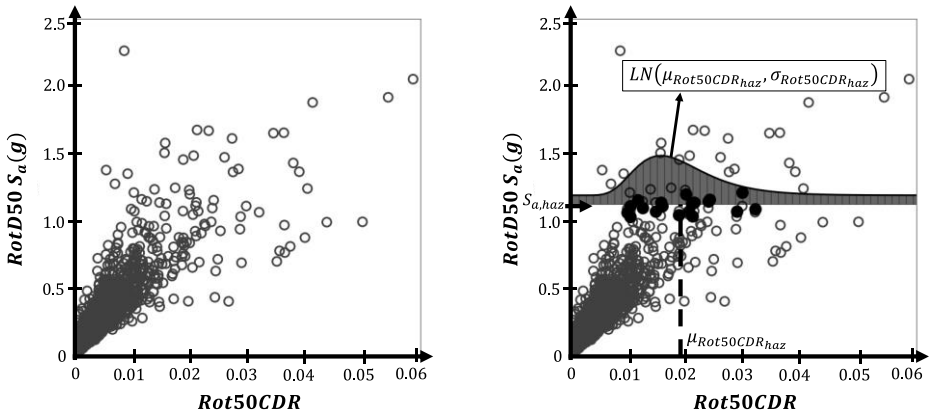

Fig 3- RotD50 S_a (IM) vs. Rot50CDR (EDP) for bridge A at the CCP site

Six values of *n* including 7, 9, 11, 13, 15 and 17 are tested along with four values of *m* which include, 3 (increment of 60°), 4 (increment of 45°), 6 (increment of 30°), and 12 (increment of 15°). For each of the 24 (6 values of $n \times 4$ values of *m*) combinations of *n* and *m*, ten trials of ground motion simulation and NLTHA are conducted to make the conclusions statistically robust. It is important to note that irrespective of the value of *m*, the EDP associated with a ground motion is always *Rot50CDR*, *i.e.*, the median value of the *m* CDRs obtained from *m* rotations of the two components of ground motion. This means that for each i^{th} ground motion the $Rot50CDR_m^i$ is obtained using Eq 1. This is done for *n* ground motions leading to a vector of $Rot50CDR_m^i$ as expressed in Eq 2 where the subscript contains *n* and *m* representing the number of ground motions (hence the number of *Rot50CDR* EDPs in the vector) and the number of intercept angles that the *Rot50CDR* EDPs are obtained from.

Furthermore, for each combination of *n* and *m*, ten sets of *n*×1 vectors of $\boldsymbol{Rot50CDR}_{n,m}$ are obtained and their average statistics are tested against the lognormal population distribution of $Rot50CDR_{haz}$. The test is conducted in two-fold; firstly, a *Hypothesis T-Test* is conducted to test the match between average sample statistics and the population mean $\mu_{Rot50CDR_{haz}}$, and secondly, the whole sample distributions are tested against the population distribution for entropy loss using *Kullback-Leiber* (*KL*) divergence. While the first test only compares the central value of responses of the two distributions, the second compares the probability distributions for information loss.

$$\boldsymbol{Rot50CDR}_{n,m} = \left\{Rot50CDR_m^i\right\} \; where \; \begin{cases} i \in \{1, 2, \ldots., n\} \\ n \in \{7,\ 9, 11, 13, 15, 17\} \\ m \in \{3, 4, 6, 12\} \end{cases} \tag{2}$$

5.1. Hypothesis T-Test

Table 3- Description of Statistical Indicators (*SI*) of Rot50CDR

$\boldsymbol{Rot50CDR}_{n,m}^{SI}$	**Description**
$Rot50CDR_{n,m}^{Mean}$	Mean of *n* values *Rot50CDR* (from *m* intercept angles)
$Rot50CDR_{n,m}^{Median}$	Median of *n* values *Rot50CDR* (from *m* intercept angles)
$Rot50CDR_{n,m}^{Median+1}$	Next higher value to the median of *n* values *Rot50CDR* (from *m* intercept angles)
$Rot50CDR_{n,m}^{Median-1}$	Next lower value to the median of *n* values *Rot50CDR* (from *m* intercept angles)
$Rot50CDR_{n,m}^{3rd}$	3rd highest value among the *n* values *Rot50CDR* (from *m* intercept angles)

Most of the simplified statistical tools are mainly based on correctly estimating the central value of the true distribution using the central value of the sample. Hence in this study, the first test is conducted to determine the minimum value of $n \times m$ that on average for ten trials, achieve a sample statistic that is statistically equivalent to the true mean $\mu_{Rot50CDR_{haz}}$. Since the aim here is to match only the true mean $\mu_{Rot50CDR_{haz}}$, different types of statistics of the *n* number of sample *Rot50CDR* EDPs are tested to achieve the $\mu_{Rot50CDR_{haz}}$. The statistics that are tested include: *mean*, *median*, *3rd largest*, *median*+1, and *median*-1 of the *n* number of sample *Rot50CDR* EDPs. For example, if *n* = 9, the 9 values of *Rot50CDR* EDPs are sorted in ascending order; *median* denotes the 5th value, *median*+1 represents the 6th value, *median*-1 represents the 4th value and *3rd largest* corresponds to the 7th value in the order. The statistics of the *n* number of *Rot50CDR* EDPs arising from *n* ground motions with *m* number of equally spaced intercept angles are generally represented as $Rot50CDR_{n,m}^{SI}$ where *SI* represents the statistical indicator (*mean*, *median*, *3rd largest*, *median*+1, and *median*-1), *n* is the number of ground motions and *m* is the number of ground motion intercept angles used in obtaining the estimate. This is briefly tabulated in Table 3.

The mean and standard deviation of the $Rot50CDR_{n,m}^{SI}$ for the 10 trials are computed and termed as $\overline{Rot50CDR_{n,m}^{SI}}$ and $s_{n,m}^{SI}$. The statistical equivalence of $\overline{Rot50CDR_{n,m}^{SI}}$, for each statistical indication (*SI*), to the $\mu_{Rot50CDR_{haz}}$ is tested through *Hypothesis T-Test*. The *t-Test* involves specifying a Null Hypothesis (H_0), which is statistically tested by calculating the *t-score* of the H_0 using the *t-distribution* and comparing its probability against a specified significance level (α). If the probability of *t-score* (*i.e. p-value*) is less than the specified significance α, then the Null Hypothesis (H_0) is rejected. The *t-score* is calculated using Eq 3, where *N* represents the number of samples (=10), and α of 0.05 (5%) is used.

$$t - score = \frac{\overline{Rot50CDR_{n,m}^{SI}} - \mu_{Rot50CDR_{haz}}}{s_{n,m}^{SI} \Big/ \sqrt{N}} \tag{3}$$

The values of *n* and *m* that satisfy the requirements of the *t-Test* and lead to the least number of simulations (*i.e.*, least $n \times m$) are chosen as the optimal values of *n* and *m*. Based on the results of all simulations it was

noticed that *median*+1 statistic deemed suitable for all bridges to represent their $\mu_{Rot50CDR_{haz}}$ for each site. Furthermore, for the two-spanned bridges (*i.e.* Bridge A and Bridge B), $n = 9$ and $m = 6$ (which means intercept angles from 0° to 150° with 30° increment) are selected as the optimal values, while for Bridge C, $n = 11$ and $m = 6$ (which means intercept angles from 0° to 150° with 30° increment) are sufficient to statistically represent the $\mu_{Rot50CDR_{haz}}$. Furthermore, for bridge F, $n = 11$ and $m = 13$ (which means intercept angles from 0° to 180° with 15° increment). Since Bridge F is curved, the response of 180° is not equal to the response of 0°; hence 180° is included. An example of the *t-Test* for the CCP site for Bridge A for the proposed statistic of *median+1* is provided in Fig 4. Fig 4a shows the variation *p-value* with respect to the changing values of n and m. As can be seen from the figure, $n = 9$ and $m = 6$, which means $n \times m = 54$ simulations are the least number of simulations required to obtain a statistically equivalent EDP to the $\mu_{Rot50CDR_{haz}}$. Fig 4b further portrays the variation of the values of *Rot50CDR* for the 9 ground motions for the 10 trials of simulations with respect to $\mu_{Rot50CDR_{haz}}$. The dark filled circles in the plot show the *Rot50CDR* for the selected statistic of *median*+1. As can be seen from the figure, the *median*+1 (6th largest among 9) *Rot50CDR* for the 10 trials lies quite close to the $\mu_{Rot50CDR_{haz}}$ which was statistically confirmed by the hypothesis test. The final proposed values of the number of ground motions (n) and equally spaced intercept angles (m) along with the corresponding intercept angle increments are tabulated in Table 4.

Table 4- Proposed number of simulations to statistically estimate $\mu_{Rot50CDR_{haz}}$

Bridge	**Number of Ground Motions (n)**	**Number of Equally Spaced Intercept Angles (m)**	**Intercept Angle Increment**
A	9	6	30° (0° to 150°)
B	9	6	30° (0° to 150°)
C	11	6	30° (0° to 150°)
F	11	13	15° (0° to 180°)

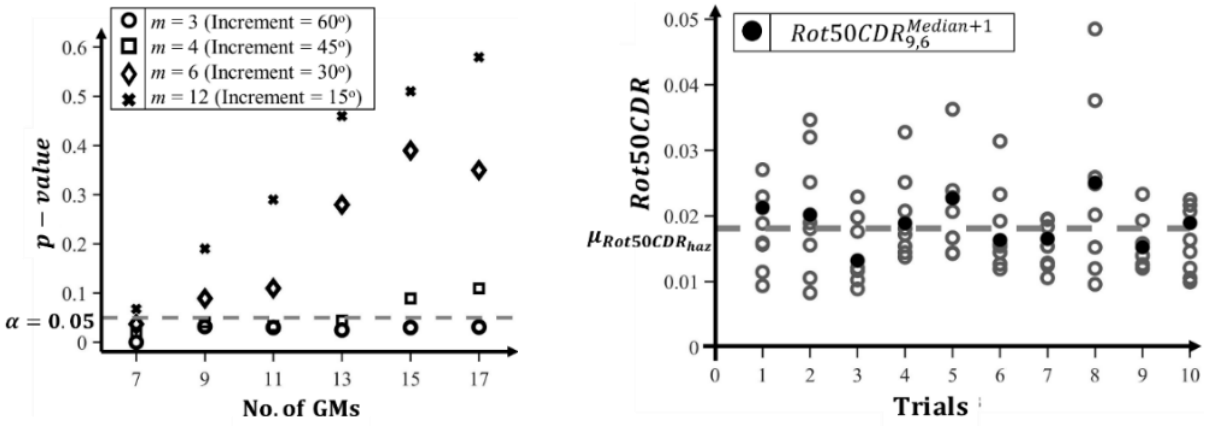

(a) (b)

Fig 4- (a) Results of hypothesis tests for all $m \times n$ for bridge A at CCP site, (b) *Rot50CDR*s for $n = 9$ GMs and $m = 6$ angles (30° increment) for ten trials

5.2. Kullback-Leibler (KL) Divergence Test

Apart from the central values of EDP distribution, other statistical measures of the distribution may have value for engineers and researchers. One application of such understanding is on the development of Load and Resistance Factor Design (LRFD) type equations for proportioning structural components (Fayaz and Zareian 2019). This section is concerned with identifying values of the sample p number ground motions and q number of equally spaced intercept angles that lead to a sample distribution of *Rot50CDR* that match the population distribution of $Rot50CDR_{haz}$; *Kullback-Leibler* (*KL*) *Divergence* is used to measure such equivalency. *KL Divergence* is a measure to determine the information entropy loss between two distributions. *KL Divergence*

(D_{KL}) measures the similarity between two probability distribution by aiming to identify the divergence of a probability distribution given a baseline distribution. That is, for a target distribution, P, we compare a competing distribution, Q, by computing the expected value of the log-odds of the two distributions using Eq 4. The target distribution P, in this study, is the population lognormal distribution of $Rot50CDR_{haz}$ with population mean $\mu_{Rot50CDR_{haz}}$ and deviation $\sigma_{Rot50CDR_{haz}}$.

$$D_{KL}(P||Q) = \sum_i P(i) log \frac{P(i)}{Q(i)} \tag{4}$$

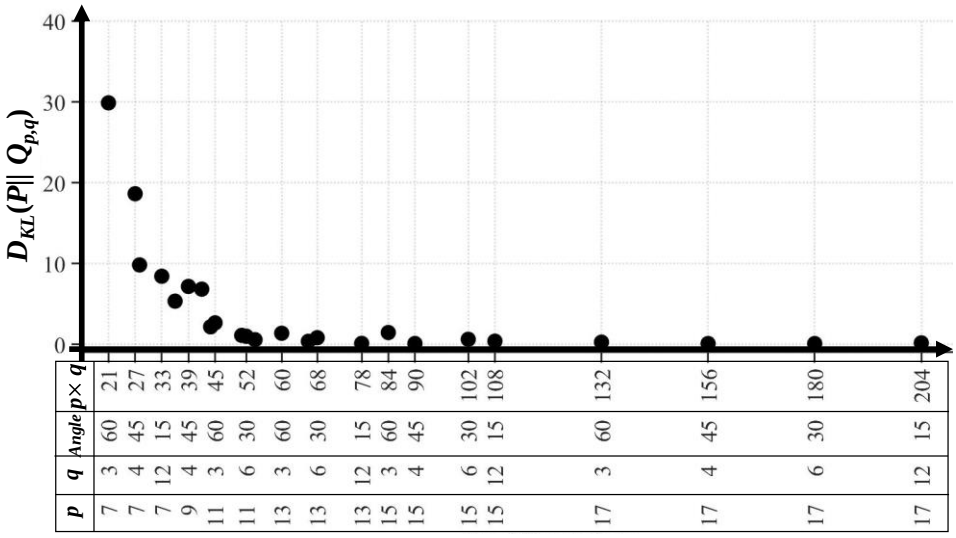

Fig 5- Results of $D_{KL}(P||\ Q_{p,q})$ for bridge A at CCP site

In this section, an attempt is made to obtain an optimal lognormal sample distribution $Q_{p,q}$ with mean using p number of ground motions and q equally spaced intercept angles from 0° to 180°. The p number of *Rot50CDR* EDPs obtained from conducting NLTHA using the sample p number ground motions with q number of equally spaced intercept angles, are assumed to follow a lognormal distribution with sample mean $\overline{Rot50CDR}_{p,q}$, and sample standard deviation $S_{p,q}$. Similar to the previous section, 24 combinations of p and q are used to compute sample distribution values. This is repeated for ten trials which leads to ten values of $\overline{Rot50CDR}_{p,q}$ and $S_{p,q}$ for each combination of p and q. The average of these ten values of $\overline{Rot50CDR}_{p,q}$ and $S_{p,q}$ are calculated and termed as $\overline{Rot50CDR}_{p,q_{avg}}$ and $S_{p,q_{avg}}$. For all 24 combinations of p and q, $\overline{Rot50CDR}_{p,q_{avg}}$ and $S_{p,q_{avg}}$ are computed and then used to compute lognormal sample distribution $Q_{p,q}$ which is compared against the true distribution P by calculating $D_{KL}(P||\ Q_{p,q})$ using Eq 4. The results of this are shown in Fig 5, where $D_{KL}(P||Q_{p,q})$ is plotted against the number of simulations (*i.e.* $p \times q$) along with their respective p, q, and Intercept angle that represents the 24 combinations for Bridge A for the CCP site. The $Q_{p,q}$ after which the rate of decrease in $D_{KL}(P||Q_{p,q})$ is deemed low for all the sites, that $Q_{p,q}$ is selected as the optimal sample distribution with the p number of ground motions and q equally spaced intercept angles. This means that the values of p and q which lead to minimal information loss while requiring the least number of simulations are selected as the optimal number of ground motions and equally spaced intercept angles to estimate the population distribution P. In the case of Bridge A, simulation of p = 13 and q = 6 (intercept angle increment = 30°) is selected as optimal sample distribution $Q_{p,q}$ to represent the population distribution P for the site. The comparison of the selected $Q_{p,q}$ against the population distribution P is shown in Fig 6. Similar plots were generated for all bridges and all sites, and the proposed values of p and q for the four bridges to represent their population distributions are given in Table 5.

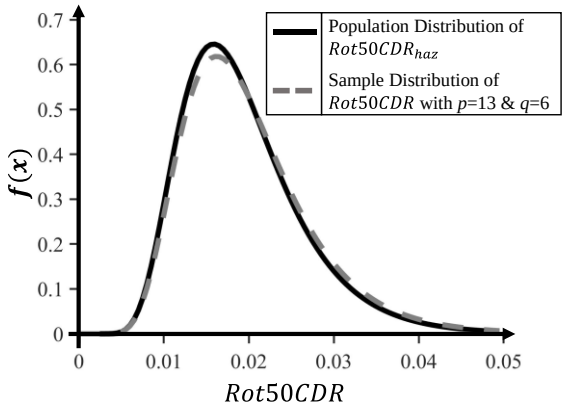

Fig 6- Comparison of Population Distribution (P) of $Rot50CDR_{haz}$ vs. Sample Distribution ($Q_{p,q}$) of $Rot50CDR$ with p= 13 GMs and q= 6 angles (30º increment angle)

Table 5- Proposed number of simulations to statistically estimate $P \sim LN(\mu_{Rot50CDR_{haz}}, \sigma_{Rot50CDR_{haz}})$

Bridge	Number of Ground Motions (p)	Number of Equally Spaced Intercept Angles (q)	Intercept Angle Increment
A	13	6	30º (0º to 150º)
B	13	6	30º (0º to 150º)
C	15	6	30º (0º to 150º)
F	17	7	30º (0º to 180º)

6. Conclusions

The current state-of-practice PEER methodology was developed to introduce a method of analysis that brings in variability arising from four random variables including Intensity Measure (IM), Engineering Demand Parameter (EDP), Damage Measure (DM), and Decision Variable (DV). Based on this, the design and analysis of structures are mainly conducted using the ground motions possessing a selected Intensity Measure (IM) and the corresponding Engineering Demand Parameter (EDP) is used as the benchmark. In the case of bridge structures, due to the asymmetry, the bi-directional components of ground motions are applied in rotations with respect to the bridge structures, and a statistic of the obtained EDPs is used for design purposes. As per the Caltrans SDC, seven or more ground motions are applied in four orientations (0, 30, 60, and 90 degrees). This leads to (4 orientations) x (7 sets of times histories) = 28 peak responses at each pertinent DOF. The bridge is then designed for the average of the 28 recorded peak responses at each degree of freedom of interest. Traditionally, recorded ground motions are used for the analysis procedure; however, recently there has been growing interest in using site-based simulated ground motions for the analysis purposes (Yoon *et al.* 2019). There, however, lacks a strong basis of how many ground motions to use and how many angles to rotate the ground motions.

This paper uses the DRD site-based ground motion simulation tool to conduct NLTHA of four ordinary bridge structures for seven sites in southern California. Catalogs of around 10,000 ground motions, corresponding to 100,000 years' time span, are simulated for each site based on the UCERF2 rupture forecast model. Using the obtained EDP-IM data and IM-hazard curves, two types of statistical tests (*Hypothesis T-Test*, and *KL Divergence*) are conducted to arrive at the optimal number of ground motions and equally spaced intercept angles that are required to match the EDPs corresponding to the IM that corresponds to the hazard level. *Hypothesis T-Test* is conducted to match only the point estimates of the expected value of EDPs, while *KL Divergence* is used to obtain the number of ground motions and angles that lead to a matching distribution of EDPs at the target IM hazard level. Based on the results of *Hypothesis T-Test*, it is derived that by using statistical indicators of *median*+1, bridges A, B, C, and F require 9, 9, 11, and 11 number of ground motions

with rotation increments of 30º, 30º, 30º, and 15º, respectively. While to match the whole distribution, using *KL Divergence*, it is concluded that bridges A, B, C, and F require 13, 13, 15, and 17 number of ground motions, all with rotation increments of 30º. Note that a windows-based GUI program called "Hazard-Targeted Time-Series Simulator (*HATSim*)" can be used to easily simulate hazard-targeted ground motions using the *DRD* model. The program is available open source at https://faculty.sites.uci.edu/pbee/links/

7. References

[1] AASHTO (2011). AASHTO Guide Specifications for LRFD Seismic Bridge Design, American Association of State Highway and Transportation Officials, 2nd Edition with 2014 Interim Revisions, Washington DC.

[2] Anastasios Kotsoglou, and Stavroula Pantazopoulou (2010). Response simulation and seismic assessment of highway overcrossing, *Earthquake Engineering and Sructural Dynamics*, Volume 3, Issue 9.

[3] Azar, S., Dabaghi, M., and Rezaeian, S., (2019). Probabilistic seismic hazard analysis using stochastic simulated ground motions. Conference Proceedings, ICASP13, South Korea

[4] Caltrans (2013). Seismic Design Criteria. Version 1.7, California Department of Transportation, Sacramento, CA.

[5] Caltrans (2019). Seismic Design Criteria. Version 2.0, California Department of Transportation, Sacramento, CA.

[6] Dabaghi, M., and Der Kiureghian, A., (2018). Simulation of orthogonal horizontal components of near-fault ground motion for specified earthquake source and site characteristics, *Earthquake Engineering & Structural Dynamics 47*, 1369–1393.

[7] Dabaghi, M., Der Kiureghian, A., Rezaeian, S., and Luco, N., (2013). Seismic hazard analysis using simulated ground motions. Paper in *Proceedings, 11th International Conference on Structural Safety and Reliability, ICOSSAR 2013*Columbia University New York, NY.

[8] Fayaz, J. and Zareian, F (2019). Reliability Analysis of Steel SMRF and SCBF Structures Considering the Vertical Component of Near-Fault Ground Motions. *ASCE- Journal of Structural Engineering*, Vol. 145, Issue 7

[9] Field, E. H., Dawson, T. E., Felzer, K. R., Frankel, A. D., Gupta, V., Jordan, T. H., . . . Wills, C. J., (2009). Uniform california earthquake rupture forecast, version 2 (UCERF 2), *Bulletin of the Seismological Society of America 99*(4), 2053-2107. doi:10.1785/0120080049.

[10] Graves, R., Jordan, T. H., Callaghan, S., Deelman, E., Field, E., Juve, G., . . . Vahi, K., (2011). Cybershake: A physics-based seismic hazard model for southern california, *Pure and Applied Geophysics 168*(3), 367-381. doi:10.1007/s00024-010-0161-6.

[11] McKenna, F., Scott, M. H., and Fenves, G. L. (2010). Nonlinear finite element analysis software architecture using object composition. *J. Comput. Civ. Eng.*, 24(1), 95-107

[12] Petersen, M. D., Frankel, A. D., Harmsen, S. C., Mueller, C. S., Haller, K. M., Wheeler, R. L., . . . Perkins, D. M., (2008). Documentation for the 2008 update of the united states national seismic hazard maps, *2331-1258*,

[13] Rezaeian, S., and Der Kiureghian, A., (2012). Simulation of orthogonal horizontal ground motion components for specified earthquake and site characteristics, *Earthquake Engineering & Structural Dynamics 41*(2), 335-353. doi:10.1002/eqe.1132.

[14] Yoon YH, Ataya S, Mahan M, Malek A, Saiidi MS, Zokaie T (2019). Probabilistic Damage Control Application: Implementation of Performance-Based Earthquake Engineering in Seismic Design of Highway Bridge Columns. *Journal of Bridge Engineering*. 2019;24(7):04019068.

